

Neurotrophic factor GDNF promotes survival of salivary stem cells

Nan Xiao,¹ Yuan Lin,² Hongbin Cao,¹ Davud Sirjani,³ Amato J. Giaccia,¹ Albert C. Koong,¹ Christina S. Kong,⁴ Maximilian Diehn,^{1,2} and Quynh-Thu Le¹

¹Department of Radiation Oncology, ²Cancer Institute and Institute for Stem Cell Biology and Regenerative Medicine, ³Department of Otolaryngology (Head and Neck Surgery), and

⁴Department of Pathology, Stanford University School of Medicine, Stanford, California, USA.

Stem cell-based regenerative therapy is a promising treatment for head and neck cancer patients that suffer from chronic dry mouth (xerostomia) due to salivary gland injury from radiation therapy. Current xerostomia therapies only provide temporary symptom relief, while permanent restoration of salivary function is not currently feasible. Here, we identified and characterized a stem cell population from adult murine submandibular glands. Of the different cells isolated from the submandibular gland, this specific population, Lin⁻CD24⁺c-Kit⁺Sca1⁺, possessed the highest capacity for proliferation, self renewal, and differentiation during serial passage in vitro. Serial transplantations of this stem cell population into the submandibular gland of irradiated mice successfully restored saliva secretion and increased the number of functional acini. Gene-expression analysis revealed that glial cell line-derived neurotrophic factor (*Gdnf*) is highly expressed in Lin⁻CD24⁺c-Kit⁺Sca1⁺ stem cells. Furthermore, GDNF expression was upregulated upon radiation therapy in submandibular glands of both mice and humans. Administration of GDNF improved saliva production and enriched the number of functional acini in submandibular glands of irradiated animals and enhanced salisphere formation in cultured salivary stem cells, but did not accelerate growth of head and neck cancer cells. These data indicate that modulation of the GDNF pathway may have potential therapeutic benefit for management of radiation-induced xerostomia.

Introduction

Xerostomia is the condition of severe hyposalivation resulting from damage of salivary glands from medications, systemic diseases (such as diabetes and Sjögren syndrome), and radiotherapy (RT) for head and neck cancer (HNC). More than 30,000 people in the United States are diagnosed with HNC annually (1); most of these patients receive RT as part of their treatment (2). Despite the widespread application of intensity-modulated RT (IMRT) to spare the parotid glands during HNC treatment, submandibular glands (SMG) are often damaged due to their proximity to the regional nodes, which are often involved in HNC. Consequently, over 80% of HNC patients treated with RT suffer from xerostomia, which severely impairs their quality of life (3). Current treatment options for RT-related xerostomia are limited and mainly focus on temporary symptom improvement (4). Stem cell (SC) therapy, in contrast, offers the possibility of permanently restoring function of the damaged glands and is therefore more attractive than existing therapeutic strategies.

The first cell-surface marker used to isolate putative salivary SCs (SSCs) from murine (5) and human SMG (6) was c-Kit. Other markers that have been used to identify SSCs include Sca1 (5, 7), Thy-1 (8), integrin $\alpha_6\beta_1$, (9, 10), and CD34 (11). The first in vivo transplantation assay used murine c-Kit⁺ cells from SMG. When

transplanted into irradiated recipient SMGs, c-Kit⁺ cells partially restored the saliva secretion in these mice (5). One major drawback of using a single cell-surface marker for SSC identification is the large heterogeneity within the isolated cell population due to contamination by hematopoietic cells and nonstem epithelial cells. Consequently, the purity of isolated SSCs, their optimal function, and their gene expression remain to be further elucidated.

By including a combination of cell-surface markers to select primarily for epithelial SCs while excluding hematopoietic lineages, we were able to obtain a much purer population of SSCs from adult mouse SMG. The Lin⁻CD24⁺c-Kit⁺Sca1⁺-enriched SSCs formed the highest number of salispheres as well as the largest and the most proliferative spheres in vitro. These cells were capable of self renewal and differentiation in vitro. Moreover, transplantation of as few as 200 to 300 Lin⁻CD24⁺c-Kit⁺Sca1⁺ cells into preirradiated SMG successfully enhanced saliva secretion and the number of functional acini on serial transplantation studies in vivo.

Improving SC survival while maintaining their regenerative properties during serial passaging in vitro and in vivo is a major challenge in SC therapy (12). Therefore, it is important to further characterize SSCs and identify the critical pathways for their survival and stemness. In this study, we also compared the gene expression of the Lin⁻CD24⁺c-Kit⁺Sca1⁺ SSC-enriched population to other subpopulations of SMG epithelial cells. We identified glial cell line-derived neurotrophic factor (*Gdnf*) as a gene that is preferentially expressed at high level in SSCs.

GDNF is a member of the GFL family, which also includes neurturin (NRTN), artemin (ARTN), and persephin (PSPN) (13, 14). GDNF has been known to play an important role in neuron

► Related Commentary: p. 3282

Conflict of interest: The authors have declared that no conflict of interest exists.

Submitted: November 4, 2013; **Accepted:** May 19, 2014.

Reference information: *J Clin Invest.* 2014;124(8):3364–3377. doi:10.1172/JCI74096.

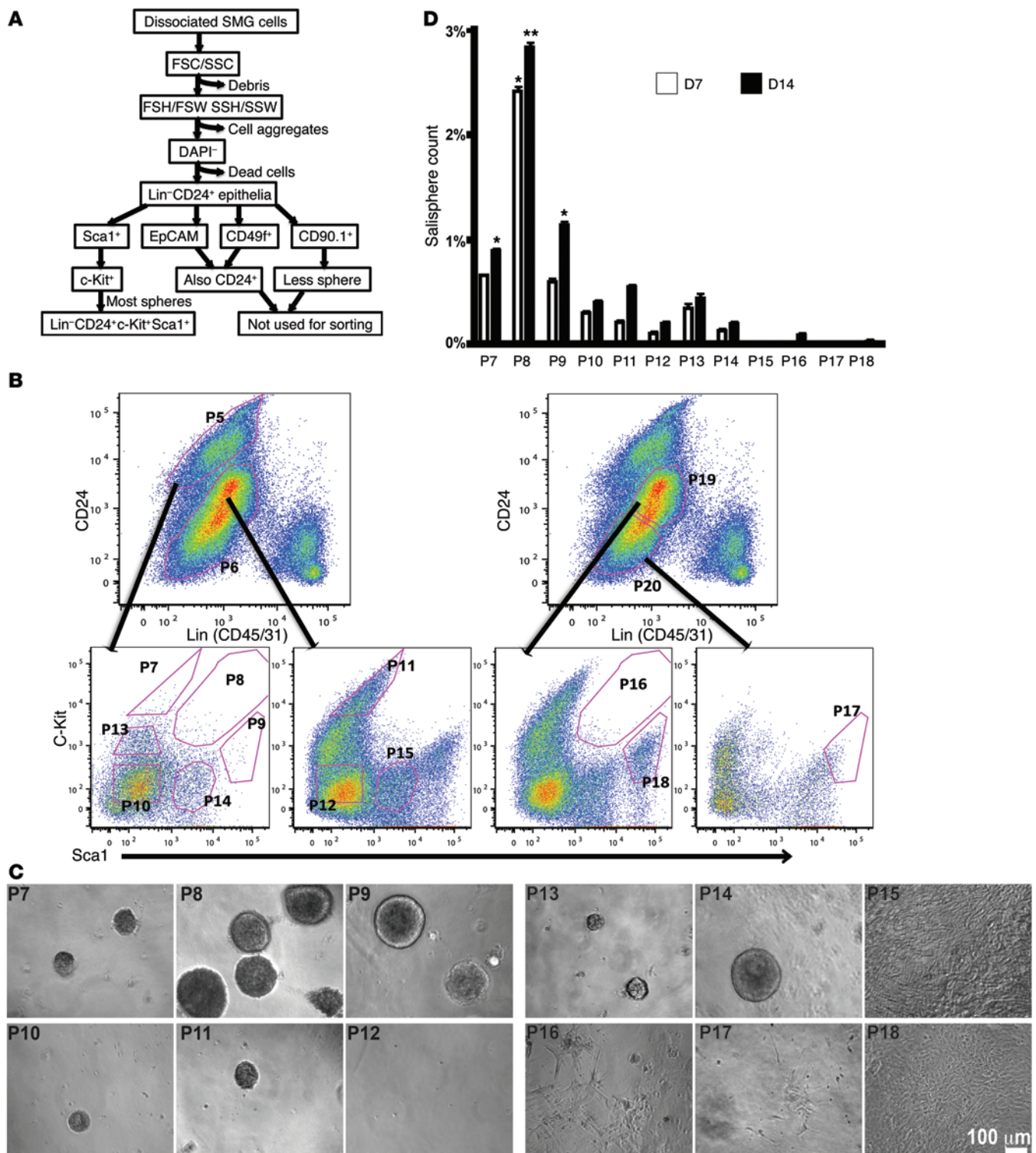


Figure 1. Identification of murine SMG SCs. (A) Flow chart of the SSC isolation strategy. FSC, forward scatter; SSC, side scatter; FSH, forward scatter height; FSW, forward scatter width; SSH, side scatter height; SSW, side scatter width. (B) Representative sorting plot for SSCs. DAPI negative, single living cells were first separated with epithelial marker CD24 and hematopoietic and endothelial lineage marker CD45/31. Lin⁻CD24^{hi} (P5), Lin⁻CD24^{lo} (P19), and Lin⁺CD24⁺ (P20) subpopulations were further separated with SC markers c-Kit and Sca1. (C) P7–P18 subpopulations were sorted and cultured on Matrigel. Representative growth patterns at D14 in vitro. Scale bar: 100 μm. (D) Quantification of salisphere number to seeding-cell number of each population at D7 and D14 in vitro. *P < 0.05; **P < 0.01, 1-way ANOVA, compared with P10 Lin⁻CD24⁺c-Kit⁺Sca1⁺ controls. n = 4. Data are presented as mean ± SEM.

survival, growth, differentiation, and migration (13, 14). It also participates in renal morphogenesis and spermatogenesis by promoting SC self renewal and proliferation (15–17). In addition, GDNF is currently being evaluated in the treatment of human Parkinson disease in clinical trials, making it a promising candidate for future SSC therapy (18, 19). We demonstrated that GDNF treatment *in vivo* either before or after RT improved saliva production in irradiated SMGs without accelerating HNC growth. GDNF treatment increased the number of surviving SCCs after RT *in vivo* and enhanced salisphere formation in culture. GDNF expression in SMG tissues increased with RT and colocalized with that of the focal adhesion kinase (FAK) in SSCs. These data together suggest that we have identified a highly enriched population of SSCs and that GDNF signaling is important for SSC survival and could thus be useful in future SC therapies.

Results

Isolation of an enriched population of murine SSCs

Defining the optimal combination of cell-surface markers for murine SSC isolation. The steps for SSC enrichment are depicted in Figure 1A. After removing clumped cells, dead cells, and cell debris, we depleted CD45⁺ and CD31⁺ hematopoietic and endothelial lineage cells (20, 21). We then enriched for epithelial cells with CD24 and EpCAM (CD326, a pan-epithelial marker) (22, 23). Since all CD24⁺ cells were EpCAM⁺, we used CD24 as the epithelial selection marker in subsequent sorting (Supplemental Figure 1A; supplemental material available online with this article; doi:10.1172/JCI74096DS1).

Because c-Kit is a well-known SC marker for many adult tissues (24, 25) and c-Kit⁺ cells have been shown to improve the function of irradiated murine SMGs (5), we used c-Kit as our anchor SC selection marker. The second SC marker that we selected was Sca1, which is an established hematopoietic SC marker (26) and was used to identify SSCs in prior studies (5, 7).

We also evaluated CD49f (integrin α_6 , another putative marker for SSC and breast cancer SC) (8, 22, 27) and CD90.1 (Thy-1, a hematopoietic stem marker) (28). Because all CD24⁺ cells were also CD49f⁺ (Supplemental Figure 1B) and CD90.1⁺ cells did not improve sphere formation over the CD24/c-Kit combination (Supplemental Figure 1C), neither marker was used in subsequent sorting.

To evaluate the sphere-forming capacity of the different cell subpopulations based on the 4 markers (CD24, c-Kit, Sca1, and lineage markers), we purified cells as depicted in Supplemental Table 1. The percentage of each population relative to the parent population is also shown in Supplemental Table 1. Representative flow profiles are shown in Figure 1B. The highest percentage of c-Kit⁺Sca1⁺ cells was noted in the CD24⁺ group (P8) (0.373%). Viable cells from 12 subpopulations of interest (P7–P18) were cultured in Matrigel. Several subpopulations were able to give rise to salispheres (Figure 1C). The Lin[−]CD24⁺c-Kit⁺Sca1⁺ (P8) population yielded the highest salisphere number (Figure 1D); in contrast, Lin[−]CD24^{lo}c-Kit⁺Sca1⁺ (P16) cells hardly formed any salisphere, indicating SSCs are derived mainly from the CD24⁺ epithelial population.

In vitro characterization of SSCs. Lin[−]CD24⁺c-Kit⁺Sca1⁺ SSC-enriched cells expressed higher levels of the SC and basal markers c-Kit, cytokeratin 5 (CK5), and CK14 compared with the Lin[−]

CD24⁺c-Kit⁺Sca1[−] cells (Supplemental Figure 2A). CK5 is a type II cytokeratin that forms a heterotetramer with type I CK14. CK5 is highly expressed in the embryonic SMG epithelial bud (29), while CK14 is a marker of basal layer epidermis (30). In contrast, SSCs expressed lower levels of acinar differentiation marker aquaporin 5 (AQP5) compared with control cells. AQP5, a water channel protein that plays a major role in saliva production and secretion, is only expressed in mature acinar cells (31). The mesenchymal marker vimentin was expressed at the same level in both enriched and nonenriched SSC populations (Supplemental Figure 2A).

Salispheres from Lin[−]CD24⁺c-Kit⁺Sca1⁺ SSC-enriched cells actively proliferated for at least 14 days *in vitro*, as indicated by Ki67 staining (Figure 2A). In addition, CK5 and CK14 partially colocalized in day 7 (D7) and D14 salispheres (Figure 2B). These results indicated that Lin[−]CD24⁺c-Kit⁺Sca1⁺ SSC-enriched cells expressed markers of basal layer epithelium and actively proliferated *in vitro*.

To show that Lin[−]CD24⁺c-Kit⁺Sca1⁺ SSC-enriched cells could differentiate *in vitro*, we stained the spheres for acinar marker AQP5, ductal luminal epithelial marker CK8 (32), and ductal basal epithelial marker CK14. AQP5 expression was patchy on D7 and D14 spheres and became more confluent on D21 spheres (Figure 2C). A similar expression pattern was noted for amylase α , which is a protein secreted by acinar cells (Figure 2D). CK8 and CK14 showed partial colocalization in D7 salispheres. CK8 was more dominantly expressed in the sphere center at D21, while CK14 was highly expressed in the sphere periphery (Figure 2E), a pattern that mimics the expression of these 2 cytokeratins in adult SMG. In contrast, the SC markers c-Kit, Sca1, and CK14 only partially colocalized with the differentiation markers amylase α or AQP5 in D21-cultured salispheres (Supplemental Figure 2B).

To prove the self-renewal ability of the SSCs *in vitro*, D7 salispheres were dissociated into single cells and recultured in Matrigel. They were able to form salispheres for at least 3 passages *in vitro*. Salispheres from the third passage continued to express the SC markers c-Kit and Sca1 up to D21 in culture (Figure 2F). MTT assays indicated that SSC salispheres were actively growing at D14 *in vitro* (Supplemental Figure 2C). These findings showed that Lin[−]CD24⁺c-Kit⁺Sca1⁺ SSC-enriched cells are capable of self-renewal, proliferation, and differentiation *in vitro*.

SSC transplantation successfully rescues SMG function after radiation. To prove that Lin[−]CD24⁺c-Kit⁺Sca1⁺ SSC-enriched cells could proliferate and differentiate *in vivo*, we injected SSCs isolated from male GFP mice directly into the SMG of the female non-GFP recipients. The surface marker profile of SMG cells from donor C57BL/6-Tg(UBC-GFP)30Scha/J mice showed a pattern similar to that from C57BL/6 mice (Supplemental Figure 3A). The GFP⁺ salisphere count derived from SSCs was also comparable to that of C57BL/6 mice (Supplemental Figure 3, B and C). To test whether the Lin[−]CD24⁺c-Kit⁺Sca1⁺ SSC-enriched cells can successfully rescue the function of SMG, the recipient mice received 15 Gy irradiation to the SMG before transplantation. As previously reported, 15 Gy irradiation largely destroyed the acini in murine SMGs (5, 11). As controls, Lin[−]CD24⁺c-Kit⁺Sca1[−] cells and unsorted bulk SMG cells were transplanted into irradiated SMGs of 2 other mouse cohorts. Stimulated saliva secretion was recorded over time to evaluate SMG function (Figure 3A).

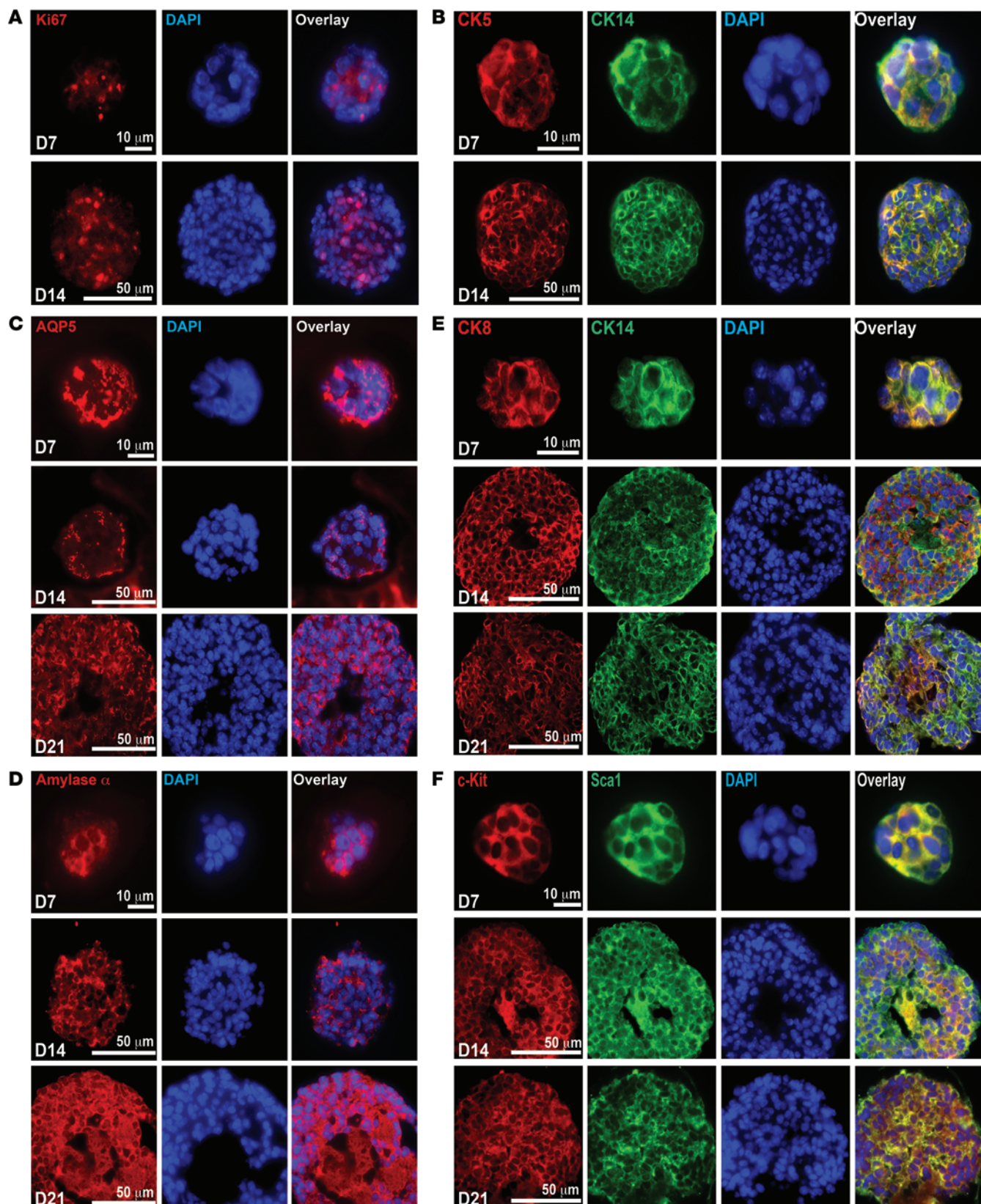


Figure 2. SSCs form salispheres and proliferate and differentiate in vitro. (A) Sorted SSCs grew into salispheres in vitro. Marker Ki67 indicates active proliferation. (B) Embryonic SSC marker CK5 and basal epithelial marker CK14 colocalized in D7 salispheres. CK5 and CK14 showed partial colocalization in D14 salispheres. (C) Acinar marker AQP5 was expressed in D7, D14, and D21 salispheres. (D) Acinar marker amylase α was expressed in D7, D14, and D21 salispheres. (E) Luminal epithelial marker CK8 partially colocalized with CK14 in D7 salispheres, but became more concentrated in the center as the spheres grew (D21). CK14 was highly expressed in the periphery of the salispheres. (F) D7, D14, and D21 salispheres from the third passages of SSCs all expressed SC markers c-Kit and Sca1. Scale bars: 10 μm (D7); 50 μm (D14); 50 μm (D21).

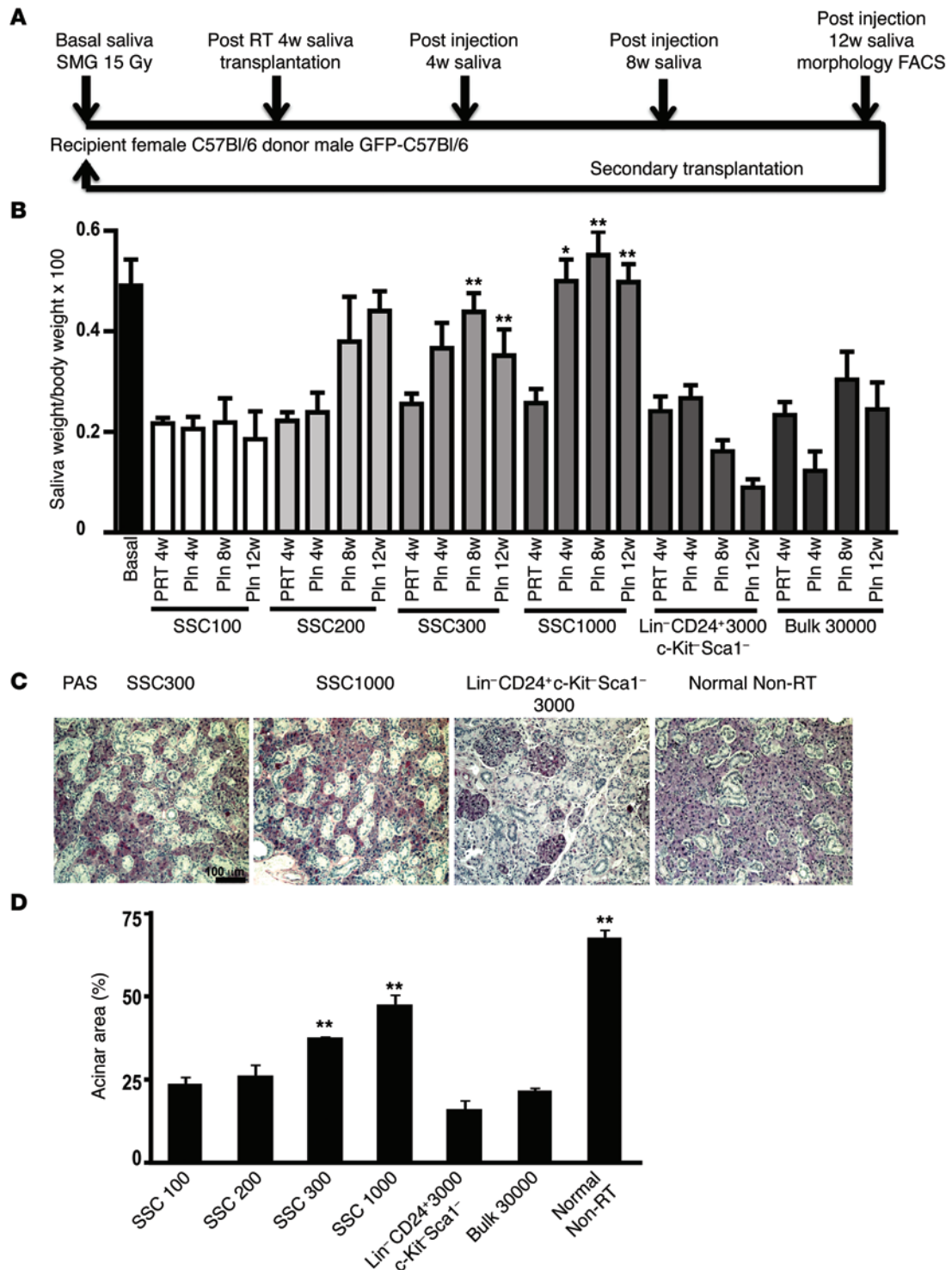


Figure 3. SSC transplantation successfully rescues SMG function after irradiation. (A) Experiment schema. (B) Total stimulated saliva secretion measured before irradiation (basal), 4 weeks after radiation treatment (PRT 4w), and 4, 8 and 12 weeks (Pln 4w, Pln 8w, Pln 12w) after SSC injection in mice receiving 100 SSCs ($n = 7$), 200 SSCs ($n = 8$), 300 SSCs ($n = 10$), 1,000 SSCs ($n = 10$), 3,000 Lin⁻CD24⁺c-Kit⁻Sca1⁻ cells ($n = 10$), and 30,000 unsorted bulk submandibular cells ($n = 5$). * $P < 0.05$; ** $P < 0.01$, 1-way ANOVA, compared with Lin⁻CD24⁺c-Kit⁻Sca1⁻ control at the same time point. (C) PAS staining of SMG at 13 weeks after SSC injection. PAS-positive cells are functional acinar cells. Scale bar: 100 μ m. (D) Quantification of the acinar area to total SMG area indicates the rescue effect of SSC transplantation. ** $P < 0.01$, 1-way ANOVA, compared with Lin⁻CD24⁺c-Kit⁻Sca1⁻ control, $n = 10$. Data are presented as mean \pm SEM.

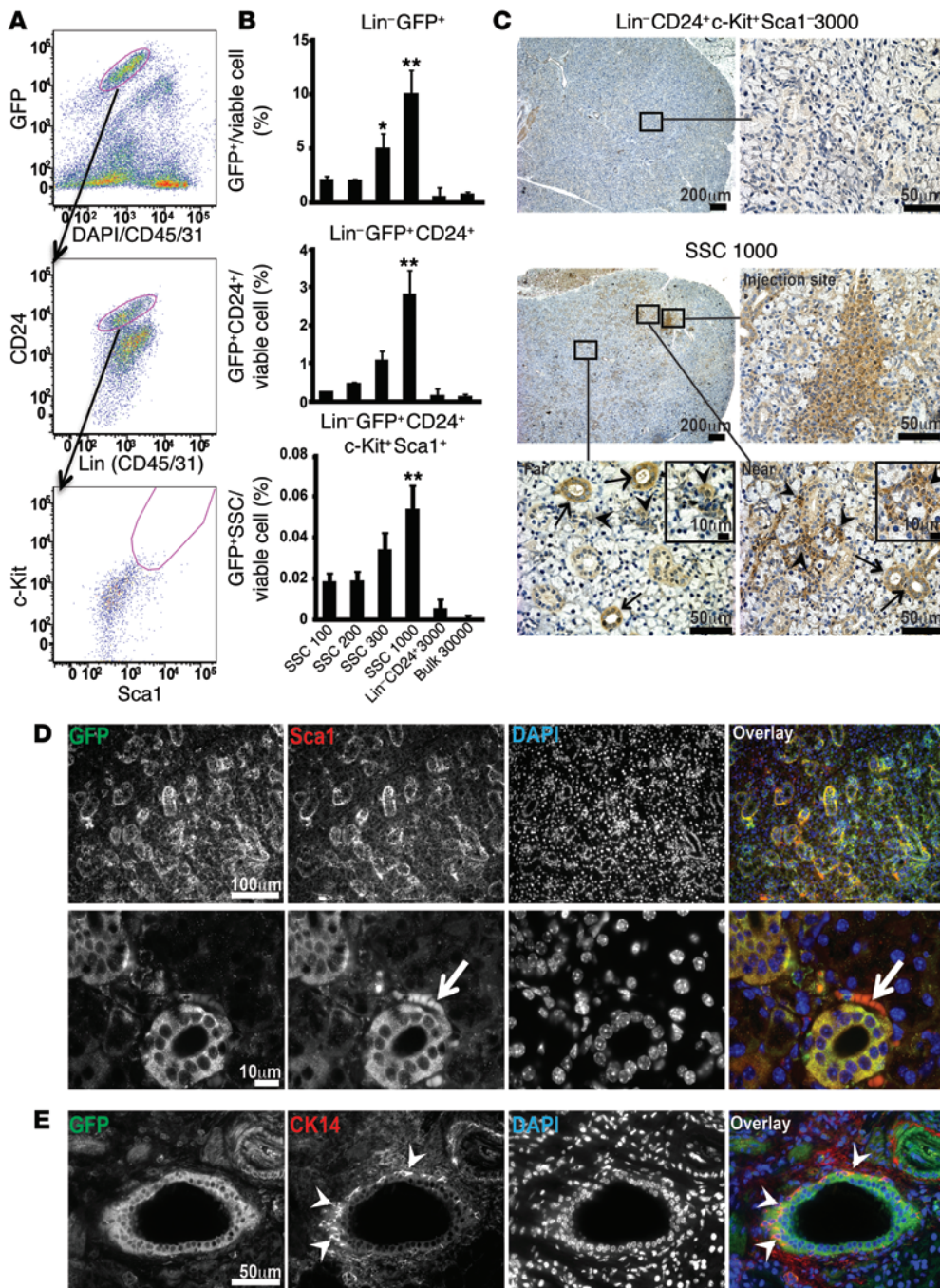


Figure 4. SSCs derived from GFP donor mice proliferate and differentiate in recipient mice. (A) Representative flow plot of recipient SMG at 13 weeks after GFP⁺ SSC injection. GFP donor SSCs differentiated into CD24⁺ epithelial and CD24^{lo} cells as well as c-Kit⁺Sca1⁺ SSCs. (B) Quantification of percentage of GFP⁺ cells (Lin⁻GFP⁺), percentage of GFP⁺ epithelial cells (Lin⁻GFP⁺CD24⁺), and percentage of GFP⁺ SSCs (Lin⁻GFP⁺CD24⁻c-Kit⁺Sca1⁺) in viable cells for the different cohorts of recipient mice in Figure 3. *n* = 7, 8, 8, 9, 9, 5 for different cohorts, respectively. **P* < 0.05; ***P* < 0.01, 1-way ANOVA, compared with 3,000 Lin⁻CD24⁻c-Kit⁻Sca1⁻ control group cells. Data are presented as mean ± SEM. (C) Immunohistochemical staining of GFP in SMG transplanted with 3,000 Lin⁻CD24⁻c-Kit⁻Sca1⁻ cells or 1,000 SSCs. The magnified views are shown correspondingly. Arrows point to secretory ducts, and arrowheads point to acini. Scale bars: 200 μm (left, top two panels); 50 μm (bottom left panel, right panels); 10 μm (insets). (D) Immunofluorescent staining of GFP and Sca1 (red) in SMG transplanted with 1,000 SSCs. Arrows point to hematopoietic cells in a blood vessel adjacent to a duct. These cells are positive for Sca1 but negative for GFP. Scale bars: 100 μm (upper panels); 10 μm (lower panels). (E) Immunofluorescent staining of GFP and CK14 (red) in SMG transplanted with 1,000 SSCs. Arrowheads point to GFP and CK14 dual-positive cells located at the basal layer of the secretory ducts in SMG. Scale bar: 50 μm.

Injection of as few as 200 Lin⁻GFP⁺CD24⁺c-Kit⁺Sca1⁺ SSC-enriched cells partially rescued saliva secretion at 8 weeks after transplantation, but the difference did not reach statistical significance. Injection of 300 SSCs significantly improved the saliva secretion at 8 weeks after transplantation when compared with the 3,000 Lin⁻CD24⁻c-Kit⁻Sca1⁻ cells injected in mice at the same time point (*P* < 0.01). Injection of 1,000 SSCs showed an even earlier rescue effect seen at 4 weeks after SSC transplantation (*P* < 0.05) (Figure 3B). This dose-response relationship, correlating the number of SSCs implanted with improved salivary gland function, strongly indicates that Lin⁻GFP⁺CD24⁺c-Kit⁺Sca1⁺ SSC-enriched cells were responsible for reconstituting saliva secretion. Based on the flow analysis, the frequency of SSC-enriched

cells in normal murine SMG was around 0.05% (Figure 1C). The number of SSCs in 30,000 unsorted bulk cells was around 15. The presence of few SSCs in the unsorted bulk cells likely accounted for the partial rescue effect noted at 8 to 12 weeks in this group. There was no rescue of saliva secretion in the Lin⁻CD24⁻c-Kit⁻Sca1⁻ control group (Figure 3B).

PAS staining, which highlights functional acini, confirmed that there were more functional acini in SMG transplanted with SSCs than with the Lin⁻CD24⁻c-Kit⁻Sca1⁻ (Figure 3C and Supplemental Figure 4). Quantification of intact acinar areas (normalized to total SMG area) showed approximately 37.6% and 47.5% acini in SMGs injected with 300 SSCs and 1,000 SSCs, respectively, compared with 16.1% acini in SMGs injected with Lin⁻CD24⁻c-Kit⁻Sca1⁻ con-

Table 1. Short list of genes validated by qPCR

Gene symbol	Gene name	GenBank accession no.	Microarray fold change	qPCR fold change
<i>Ly6d</i>	Lymphocyte antigen 6 complex, locus D	NM_010742	4.50	5.94
<i>Wnt10a</i>	Wingless related MMTV integration site 10a	NM_009518	4.44	3.4
<i>Smr3a</i>	Submaxillary gland androgen regulated protein 3A	NM_011422	4.20	3.19
<i>Nrxn1</i>	Neurexin I	NM_020252	4.10	2.58
<i>Krt17</i>	Keratin 17	NM_010663	3.86	5.62
<i>Krt14</i>	Keratin 14	NM_016958	3.28	5.42
<i>Il18r1</i>	IL-18 receptor 1	NM_008365	3.28	5.58
<i>Ngfr</i>	Nerve growth factor receptor (TNFR superfamily, member 16)	NM_033217	3.27	5.19
<i>Krt5</i>	Keratin 5	NM_027011	3.18	4.14
<i>Ly6a(Sca1)</i>	Lymphocyte antigen 6 complex, locus A	NM_010738	3.01	2.95
<i>Camk4</i>	Calcium/calmodulin-dependent protein kinase IV	NM_009793	3.00	2.93
<i>Krt15</i>	Keratin 15	NM_008469	2.79	5.03
<i>Fgfr3</i>	FGF receptor 3	NM_008010	2.70	3.92
<i>Aldh3a1</i>	Aldehyde dehydrogenase family 3, subfamily A1	NM_007436	2.50	3.75
<i>Gdnf</i>	Glial cell line-derived neurotrophic factor	NM_010275	2.33	4.11
<i>Wnt6</i>	Wingless-related MMTV integration site 6	NM_009526	2.14	1.7
<i>Krt8</i>	Mus musculus keratin 8 (Krt8), mRNA [NM_031170]	NM_031170	-0.20	0.57
<i>Aqp5</i>	Aquaporin 5	NM_009701	-3.34	-1.5

tol cells ($P < 0.01$) (Figure 3D). Of note, the percentage of intact acinar in unirradiated SMG ranged from 60% to 70%.

Transplanted SSCs proliferate and differentiate in recipient murine SMGs. Flow analysis indicated that there were significantly more Lin⁻GFP⁺ cells in the 1,000 SSC-transplanted group compared with the 3,000 Lin⁻CD24⁺c-Kit⁺Sca1⁻ control group (Figure 4, A and B). GFP⁺ cells from donor mice successfully differentiated into Lin⁻CD24⁺ cells, Lin⁻CD24^{lo} cells, and Lin⁻CD24⁺c-Kit⁺Sca1⁺ cells (Figure 4A). The percentages of Lin⁻CD24⁺ epithelial and Lin⁻CD24⁺c-Kit⁺Sca1⁺ SSC-enriched cells (in viable cells) were significantly higher in the 1,000 SSC-transplanted group compared with the control group (Figure 4B).

Immunohistochemical (IHC) staining of GFP further confirmed that there were more GFP⁺ cells in the 1,000 SSC-transplanted SMG (Figure 4C). Although GFP⁺ SSCs tended to aggregate around the injection site, we also noted GFP⁺ cells in regions distant from the injection site at 12 weeks after transplantation. The multipotency of the SSCs was proved by the fact that GFP⁺ SSCs differentiated into both GFP⁺ secretory ducts (Figure 4C, arrows) and GFP⁺ acini (Figure 4C, arrowheads) at regions near and far from the transplantation site. These results were further confirmed by immunofluorescence (IF) staining. A subset of cells expressed GFP as well as the SC marker Sca1 (Figure 4D) and basal epithelial marker CK14 (Figure 4E, arrowheads), indicating that some GFP⁺ cells maintained SSC features and remained undifferentiated at the basal epithelial layer, where SSCs are normally found. Moreover, GFP⁺ SSCs were distinct from endogenous hematopoietic cells, which were GFP negative but Sca1 positive (Figure 4D, arrow).

GFP⁺ SSCs isolated from primary recipients successfully rescue SMG function after radiation in secondary recipients. To confirm that the Lin⁻GFP⁺CD24⁺c-Kit⁺Sca1⁺ SSC-enriched cells could self-renew in vivo after transplantation into recipient SMGs, we performed a serial transplantation study. GFP⁺ SSCs were isolated

from the SMGs of the primary recipients and transplanted into irradiated SMGs of the secondary recipients (Figure 3A). 250 Lin⁻GFP⁺CD24⁺c-Kit⁺Sca1⁺ SSC-enriched cells successfully rescued saliva secretion in the secondary recipients (Supplemental Figure 5A). Similar to what was found in the primary recipients, Lin⁻GFP⁺ cells were able to differentiate into Lin⁻CD24⁺, Lin⁻CD24^{lo}, and Lin⁻CD24⁺c-Kit⁺Sca1⁺ SSC-enriched populations (Supplemental Figure 5B). PAS staining confirmed that SMG morphology was partially rescued in the secondary recipients (Supplemental Figure 5C). GFP immunolabeling showed that GFP⁺ SSCs successfully proliferated in the secondary recipients and differentiated into secretory ducts (Supplemental Figure 5D, arrows) and acini (Supplemental Figure 5D, arrowheads). CK14 expression likewise colocalized with GFP in the secretory ducts (Supplemental Figure 5E, arrowheads). Finally, isolated SSCs from secondary recipients were able to grow into salispheres, which expressed SC marker Sca1 (Supplemental Figure 5F).

Taken together, these results confirmed that Lin⁻GFP⁺CD24⁺c-Kit⁺Sca1⁺ SSCs were able to self-renew in vivo in serial transplantation. The progenies derived from GFP⁺ SSCs were able to proliferate and differentiate in vivo for at least 6 months after the original isolation. Based on these data, we believe that we have isolated a relatively pure SSC population for further characterization.

Gene-expression analysis of Lin⁻CD24⁺c-Kit⁺Sca1⁺ SSC-enriched population

To investigate the molecular characteristics of SSCs, we performed gene-expression analysis of a Lin⁻CD24⁺c-Kit⁺Sca1⁺ SSC-enriched population compared with Lin⁻CD24⁺c-Kit⁺Sca1⁻ cells using the Agilent SurePrint G3 Mouse GE microarray platform, which contains 39,430 Entrez Gene RNAs and 16,251 long intergenic non-coding RNAs (lncRNAs). The 197 genes, which showed more than 2-fold elevation in the Lin⁻CD24⁺c-Kit⁺Sca1⁺ SSC-enriched popula-

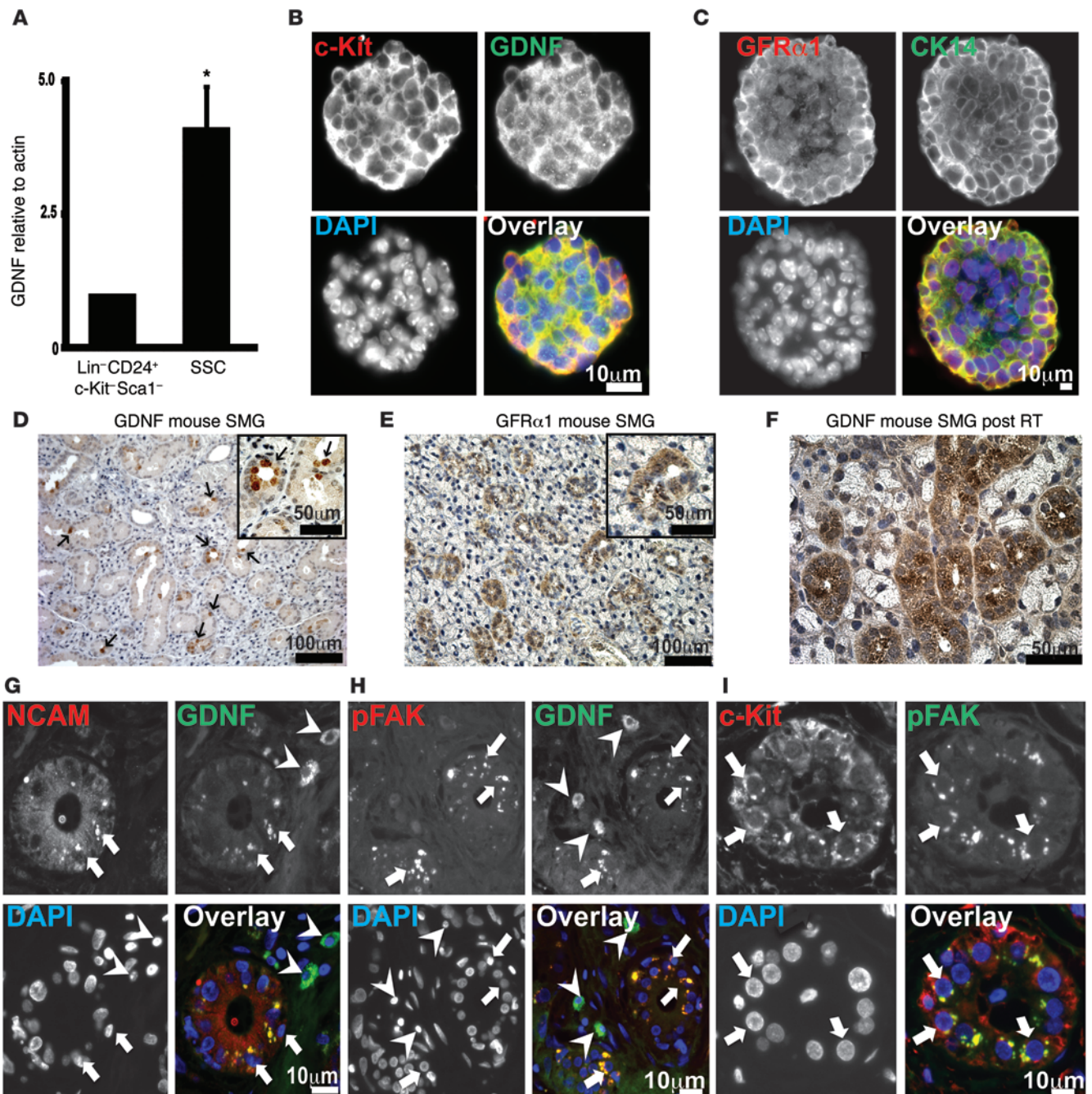


Figure 5. GDNF expression in salispheres and SMG tissues. (A) qPCR showed *GDNF* mRNA was highly expressed in SSCs compared with *Lin⁻CD24⁺c-Kit⁻Sca1⁻* cells. * $P < 0.05$, t test. $n = 3$. Data are presented as mean \pm SEM. (B) GDNF colocalized with SC marker *c-Kit* in the salisphere. Scale bar: 10 μ m. (C) *GFR α 1* colocalized with basal keratin marker *CK14* in the salisphere. Scale bar: 10 μ m. (D) GDNF and (E) its receptor *GFR α 1* were primarily expressed in the secretory duct of murine SMG by immunohistochemical staining. Scale bars: 100 μ m; 50 μ m (insets). (F) GDNF signal was elevated 9 weeks after 15-Gy radiation treatment. Scale bar: 50 μ m. (G) GDNF colocalized with *NCAM* in the ducts after irradiation in human SMG (arrows), but not in the neighboring neurons (arrowheads). (H) GDNF colocalized with *pFAK* in the ducts after irradiation in human SMG (arrows), but not in the neighboring neurons (arrowheads). (I) *pFAK* localized in *c-Kit*-positive SSCs in the ducts after irradiation in human SMG (arrows). The signals partially overlapped. Scale bar: 10 μ m (G-I).

tion, can be categorized into 30 groups through the DAVID Functional Annotation. Growth factors closely regulate SC proliferation, regeneration, and differentiation. Seven growth factors, *Klk1b3*, *Klk1b4*, *Artn*, *Ptn*, *Bmp7*, *Gdnf*, and *Cxcl12*, had elevated expression in the SSC-enriched population (Supplemental Table 2).

To confirm the gene expression profile of the functional categories with statistical significance, 75 genes were selected for quanti-

tative PCR (qPCR) validation. We focused on the genes in the functional categories of SC markers, epithelial markers, and growth factors that showed more than 2-fold elevation in the SSC-enriched population. We also included some genes without any change (5 genes) or with decreased expression (15 genes) as controls. Out of 75 genes, 18 were confirmed with qPCR in 4 independent samples (Table 1). As expected, the expression of *Sca1* and *c-Kit* was

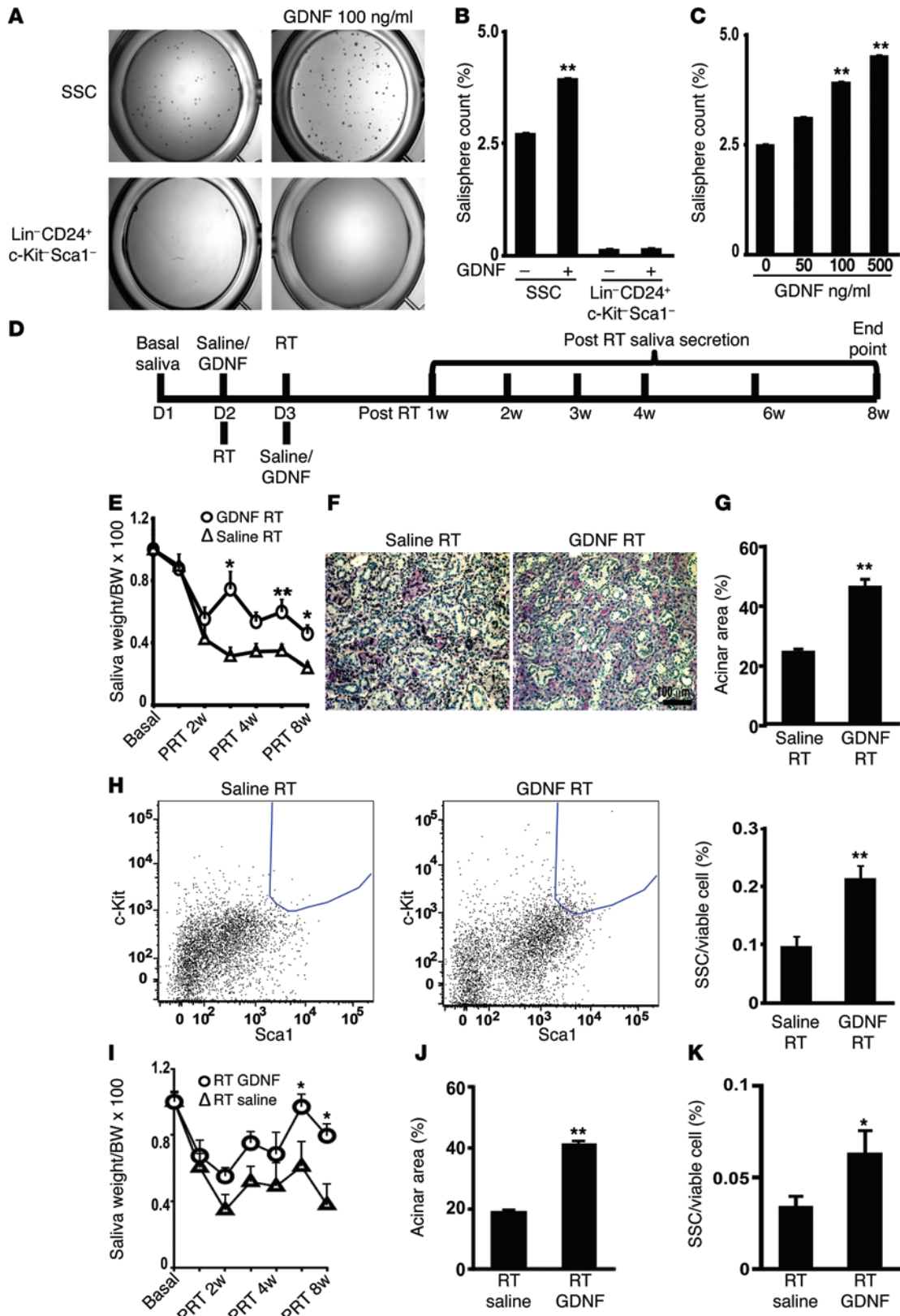


Figure 6. GDNF injection successfully rescues radiation-induced SMG

damage. (A) Treatment with GDNF increased the salisphere number in SSCs, but not in Lin⁻CD24⁺c-Kit⁻Sca1⁻ cells. (B) Quantification of salisphere number treated with or without GDNF. $**P < 0.01$, *t* test, compared with nontreated SSCs. SSC (*n* = 5); Lin⁻CD24⁺c-Kit⁻Sca1⁻ (*n* = 10). (C) GDNF increased salisphere count in a dose-dependent manner. $**P < 0.01$, *t* test, compared with nontreated SSCs (*n* = 6). (D) Experimental schema. 50 μg/mouse GDNF or saline was injected intraglandularly into SMG 1 day before (E–H) or after (I–K) 15 Gy radiation of the SMG. (E) Total stimulated saliva secretion measured before irradiation (basal), 1, 2, 3, 4, 6, and 8 weeks after radiation treatment (PRT). *n* = 10/group. $*P < 0.05$; $**P < 0.01$, *t* test. (F) PAS staining of SMG 8 weeks after RT. PAS-positive cells are functional acinar cells. Scale bar: 100 μm. (G) Quantification of the acinar area to total SMG area indicates the rescue effect of GDNF. $**P < 0.01$, *t* test. (H) Representative flow plot of SMG at 8 weeks after GDNF/saline injection. Quantification of SSC (Lin⁻CD24⁺c-Kit⁻Sca1⁺) percentage in viable cells (DAPI) indicated that GDNF significantly increased the SSC numbers. (*n* = 7/group) $**P < 0.01$, *t* test. (I) Total stimulated saliva secretion. GDNF or Saline was injected 1 day after RT (*n* = 10/group). $*P < 0.05$; $**P < 0.01$, *t* test. (J) Quantification of the acinar area to total SMG area. $**P < 0.01$, *t* test. (K) Quantification of SSC percentage in viable cells (*n* = 8/group). $*P < 0.05$, *t* test. All data are presented as mean ± SEM.

higher in SSC than in control cells. The basal keratin markers *Krt5*, *Krt15*, *Krt14* were also highly expressed in SSCs. In contrast, the expression of differentiation markers *Krt8* and *Aqp5* were lower in SSC. The Gene Expression Omnibus (GEO) access for the microarray data can be found on NCBI website (GSE46672).

The role of GDNF in SSCs

GDNF expression in salispheres and SMG tissues. Of interest is GDNF, which showed a more than 2-fold elevation in SSCs by microarray and was 4-fold higher in SSCs by qPCR when compared with the Lin⁻CD24⁺c-Kit⁻Sca1⁻ population (Figure 5A). GDNF preferentially binds to the GDNF family receptor $\alpha 1$ (GFR $\alpha 1$), which mediates the activation of the RET receptor tyrosine kinase and functions through the PI3K/AKT, MEK/ERK and SRC pathways in neurons (33, 34), ureteric buds (35, 36), and spermatogonial SCs (37). Recent studies indicated that the neural cell adhesion molecule (NCAM) and the downstream targets FYN/FAK may function as alternative pathways for GDNF in regulating axonal guidance and corneal regeneration (38–41).

In cultured salispheres, GDNF expression colocalized with the SC marker c-Kit (Figure 5B), while GFR $\alpha 1$ colocalized with the basal keratin marker CK14 (Figure 5C). In murine SMG tissues, GDNF (Figure 5D, arrows) and GFR $\alpha 1$ (Figure 5E) were located at the basal layer of the secretory duct epithelium. Similar localization was also noted in human SMG (Supplemental Figure 6, A and B). Moreover, GDNF expression overlapped with that of GFR $\alpha 1$ in mouse SMG (Supplemental Figure 6C). The expression of RET, a receptor tyrosine kinase that can be activated upon GDNF's binding to GFR $\alpha 1$, was relatively weak and did not show enrichment in the ducts (Supplemental Figure 6D). The signal of NCAM, another coreceptor, was too weak to be detected in normal SMG tissues.

In irradiated murine and human SMGs, GDNF expression was highly upregulated (Figure 5F and Supplemental Figure 6E). The coreceptor NCAM became detectable after RT and colocalized with GDNF in the secretory duct (Figure 5G, arrows), but not in the neighboring neurons (Figure 5G, arrowheads). Moreover, phosphor-FAK (pFAK), the downstream target of NCAM, was also

detected in the ducts and colocalized with both GDNF (Figure 5H, arrows) and c-Kit (Figure 5I, arrows) in irradiated SMG tissues. In contrast, the downstream target of RET, including phosphor-AKT (pAKT) (Supplemental Figure 6F) and phosphor-ERK (pERK) (Supplemental Figure 6G) did not colocalize with c-Kit in irradiated SMG tissues. These results indicated that in SSCs, GDNF and GFR $\alpha 1$ were likely to function through the interaction with the coreceptor NCAM, which then activated FAK after radiation damage to the SMG.

GDNF promotes salisphere growth in vitro. To further evaluate the role of GDNF in SSCs, we applied GDNF in vitro on SSCs. When GDNF (100 ng/ml) was added to SSCs in culture, it significantly increased salisphere-forming cell frequency, from 2.7% to 4.0%, whereas it had no effect on control Lin⁻CD24⁺c-Kit⁻Sca1⁻ cells (Figure 6, A and B). In addition, GDNF increased the salisphere number in a dose-dependent manner (Figure 6C). These data suggest that GDNF is a potential growth factor to promote SSC survival.

GDNF successfully rescues SMG after radiation. We investigated whether GDNF treatment in vivo would improve saliva production in irradiated SMGs. A single dose of 50 μg GDNF was injected directly into the SMG of each mouse 24 hours before 15-Gy irradiation. Saliva secretion was measured up to 8 weeks after RT, at the time of sacrifice (Figure 6D). When compared with control saline injection, a single GDNF injection significantly improved saliva production in irradiated mice. The rescue effect was durable, up to 8 weeks after irradiation, when the mice were euthanized for histological studies (Figure 6E). There was no difference in the body weights of GDNF and saline-injected mice, suggesting no systemic toxicity. PAS staining revealed more functional and intact acini in GDNF-treated SMGs than in saline glands (Figure 6F), translating to a larger area of intact acini in GDNF-treated mice (Figure 6G). FACS studies also showed significantly more SSCs in GDNF-treated SMGs compared with saline-treated controls (Figure 6H).

Since GDNF expression is elevated after RT, we also tested whether GDNF injection after RT would rescue the saliva production (Figure 6D). 50 μg GDNF was injected directly into the SMG of each mouse 24 hours after 15 Gy irradiation. GDNF improved saliva production after RT (Figure 6I) and increased the percentage of functional acini (Figure 6J and Supplemental Figure 7A). FACS studies again showed more SSCs in GDNF-treated SMG than the saline group (Figure 6K and Supplemental Figure 7B).

GDNF does not function as a radio protector in SMG. To rule out the possibility that GDNF acted as a general radiation protector of mature salivary cells, we investigated whether GDNF could protect rat SMG cell line SMG-C6 from radiation-induced cell damage. Clonogenic survival assay showed that GDNF treatment did not affect cell survival from radiation treatment (Supplemental Figure 8A). ROS generated during irradiation as a result of water radiolysis was not changed by GDNF treatment (Supplemental Figure 8B). The pattern of phosphor- γ H2AX after irradiation over time, which reflected radiation-induced DNA double-strand breaks, was not different with or without GDNF treatment (Supplemental Figure 8C). Although RT induced a G₁ arrest in SMG-C6 cells, there was no difference in the cell-cycle pattern with or without GDNF treatment (Supplemental Figure 8D). These data all indicated that GDNF did not act as an overall radio protector in mature salivary cells.

GDNF treatment did not accelerate HNC growth. In HNC cell line SCC 22A, 100 ng/ml GDNF applied 30 minutes before RT did not affect clonogenic survival (Supplemental Figure 9A). More importantly, intratumor injection of 50 μ g GDNF 24 hours after 12-Gy irradiation to the tumor did not affect the tumor growth delay compared with the control (Supplemental Figure 9B). These data indicated that GDNF did not modify tumor growth or response to irradiation.

Discussion

Repair and reconstitution of adult tissues depends on a small population of SCs. Adult SCs are believed to be quiescent, but become activated and drive tissue regeneration upon damage (10, 42, 43). There is an increasing interest in SC therapy to restore salivary gland function after radiation. SCs from tissues other than salivary gland, including bone marrow (7, 44–50), pancreas (51), and lacrimal gland (52), have been shown to differentiate into salivary acinar-like structures in vitro, but whether these cells can have acini function in vivo remains to be further investigated.

SCs that reside in the salivary microenvironment are programmed to differentiate into adult glands and are more likely to form functional subunits than SCs from other organs. Recently, efforts have been made to isolate a pure population of adult SSCs. Several single cell-surface markers, including c-Kit (5), Sca1 (5, 7), Thy-1 (8), integrin $\alpha_6\beta_1$ (9, 10), and CD34 (11), have been used to identify these cells. Although these subpopulations exhibited certain SC properties in vitro, only c-Kit-positive cells have been transplanted in vivo and could partially rescue saliva function. Identification of a pure SSC population will help to reduce the number of SSCs required for future therapy and will allow for better characterization of these cells.

Here, by using multiple cell-surface markers, we have identified a highly enriched population of SSCs, as demonstrated by their ability to form more spheres and rescue salivary function after irradiation in vivo with relatively few cells. More importantly, these Lin⁻CD24⁺c-Kit⁺Sca1⁺ cells can differentiate into duct and acinar structures, demonstrating multipotency and self-renewal ability both in vitro and in vivo through serial transplantation studies, up to 6 months after initial isolation.

Several pathways have been implicated in SSC regeneration, proliferation, and differentiation. These include the WNT and NOTCH signaling pathways for SC self renewal and lineage determination (53–56), ASCL3 for proliferation (57), and GSK3 β for cell differentiation (58). In addition, the SC niche clearly plays an important role in the fate of SCs (59). Many growth factors are involved in salivary gland morphogenesis during development and regeneration (60), including keratinocyte growth factor (KGF, also known as FGF7) (61), FGF10 (62–64), and EGFR (65). Our gene-expression analysis of the Lin⁻CD24⁺c-Kit⁺Sca1⁺ SSC-enriched population confirmed that several of the genes involved in SC self renewal, lineage determination, and development are differentially upregulated in these cells. These genes include Wnt members *Wnt10a* and *Wnt6*, which are involved in osteogenesis through a β -catenin-dependent mechanism (66). *Wnt6* was also implicated in inducing epithelialization of primitive endodermal cells (67). Nerve growth factor receptor (NGFR, also known as p75 and CD271), has been identified as a stem SC marker in neuron

(68), bone marrow (69), and adipose tissue (70). The keratin SC markers CK5 and CK14, which are important in maintaining epithelial proliferation (71), are highly expressed in SSCs. Keratin 15 a SC marker in the hair follicle (72), and keratin 17 could compensate for the loss of CK14 in mouse keratinocytes in maintaining cell growth (73). The role of these SSC-enriched genes in SC function will need further investigation.

Of interest are genes that have not been previously identified in SSC self renewal. One such gene is *Gdnf*, which is highly expressed in the SSC-enriched population compared with other epithelial cells. GDNF is known to play an important role in neuron survival, growth, differentiation, and migration (13, 14) and has been implicated in renal morphogenesis and spermatogenesis by promoting SC self renewal and proliferation (15–17). Recently, a GDNF family member, NRTN, was reported to promote mouse embryonic SMG regeneration (74). Our data showed that GDNF treatment resulted in enhanced SSC survival and mitigation of RT-induced functional damage in vivo. Injection of a single dose of 50 μ g GDNF into the SMG either before or after RT significantly improved saliva secretion in irradiated mice. The functional rescue was associated with a higher SSC yield in vivo when compared with saline controls. GDNF also promoted salisphere formation of SSCs in vitro in a dose-dependent manner, but did not protect differentiated acinar cells from RT damage. Our findings strongly support that GDNF did not function as a general radiation protector, but rather promoted regeneration through SSCs.

GDNF binds to GFR α 1, which mediates the activation of either the RET receptor tyrosine kinase or the NCAM in neurons. RET activates the PI3K/AKT, MEK/ERK, and SRC pathways, and NCAM activates the FYN/FAK pathway. Through these downstream targets, GDNF prevents apoptosis and promotes proliferation and differentiation in neurons (33, 34, 38–40), ureteric bud (35, 36), and spermatogonial SCs (37). Our results show that GDNF and its receptor, GFR α 1, are found primarily in SSCs, suggesting that GDNF mainly acts as an autocrine factor. The fact that radiation increased the expression of GDNF and its colocalization with NCAM and pFAK in ductal epithelium suggests that GDNF activates the NCAM/FAK pathway in SSCs after RT damage.

ETS transcription factors ETV4 and ETV5 are known downstream targets of the GDNF/RET pathway and are involved in neuronal development (75), kidney branching (76), and spermatogenesis (77). In our microarray analysis, *Etv4* and *Etv5* were not upregulated in the SSCs, but 2 other ETV family transcription factors, *Etv6* and *Etv1*, were found enriched in SSCs. However, neither *Etv6* nor *Etv1* expression showed significant changes in SSCs upon GDNF treatment. These data, coupled with the fact that GDNF did not colocalize with RET, pAKT, or pERK in either salispheres or salivary ductal cells, suggest that the RET signaling pathway may not be a significant player in the GDNF pathway in SSC.

Since GDNF is currently being evaluated for the treatment of human Parkinson disease in clinical trials (18, 19). The potential application of GDNF in improving the survival of SCCs would be readily translated to the clinic. Although our results showed that GDNF was not a general radiation protector for mature salivary cells, whether GDNF primarily promotes SSC survival and proliferation after radiation or can also promote SSC differentiation remains to be further investigated. We have shown that GDNF treatment did

not affect radiation response or tumor growth in an HNC cell line. However, since GDNF is a growth factor, its effect on promotion of salivary cancer development will need to be thoroughly studied.

In summary, we have identified a relatively pure SSC population that is capable of self renewal and functional restoration of irradiated SMG. We have also identified a growth factor, GDNF, that appears to increase the SSC population after radiation treatment and did not promote tumor growth in a HNC cell line. Manipulation of the GDNF pathway may provide a promising avenue for future SSC therapy in the clinical setting.

Methods

Animals. C57BL/6 mice and C57BL/6-Tg(UBC-GFP)30Scha/J mice were purchased from Jackson Laboratory.

Flow cytometry. SMG tissues were minced and dissociated in DMEM/F12 medium (Gibco; Invitrogen) containing collagenase I (0.025%), hyaluronidase (0.04%), CaCl₂ (6.25 mM), and 25 U/ml dispase (BD Biosciences) for 2 hours at 37°C. The dissociated cells were centrifuged at 300 g and filtered through a 400 μm Millipore filter (Millipore). After the red blood cell lysis, primary SMG cells were incubated simultaneously with anti-mouse CD24, CD45, CD31, Sca1 (eBioscience), and c-Kit antibodies (BD Biosciences) for 30 minutes on ice to determine the SC population. Cell viability was detected with DAPI (Invitrogen). Cells were sorted on a BD FACS Aria II (BD Biosciences).

Irradiation and intraglandular injection. Six- to eight-week-old female C57BL/6 mice were exposed to a single dose of 15 Gy ionized irradiation (250k Vp orthovoltage) using the IC-225 Specimen Irradiation System (Kimtron Medical). The SMGs were irradiated from the lateral side (7.5 Gy per side, total 15 Gy), with the rest of the body protected by a lead shield, as previously reported (11). Representative photographs of the procedure are shown in Supplemental Figure 10. In brief, 4 weeks after irradiation, mice were anesthetized and SMG was exposed by small incision. Sorted cells were suspended in 10 μl culture medium with 0.5% trypan blue. 5 μl of cells were injected into each side of the SMGs using a 10 μl microinjection syringe (Hamilton Co.). The skin incision was closed with surgical suture. Then 50 μg/mouse GDNF (R&D Systems) was injected through open surgery as described about.

Saliva collection. Saliva was collected for 15 minutes after 2 mg/kg pilocarpine injection (s.c.), as previously described (11). The saliva flow rate was determined at basal condition, 4 weeks after radiation (postradiation treatment [PRT] 4w), and 4, 8, and 12 weeks after cell injection (postinjection [PIIn] 4w, PIIn 8w, and PIIn 12w). The measured saliva secretion was normalized to the mouse body weight, assuming 1 g/ml density for saliva.

Microarray and analysis. Total RNA from the sorted cells was extracted with RNeasy kit (QIAGEN) following the manufacturer's protocols. Gene expression was determined with Agilent SurePrint G3 Mouse GE 8x60K arrays (Agilent Technologies) at Stanford Functional Genomics Facility and analyzed with GeneSpringGX (Agilent Technologies). The signal threshold intensity was greater than 5, baseline

transformation was made to the median of all samples and normalized to the 75th percentile shift. Genes showing more than 2-fold elevation compared with control were further categorized through the DAVID Functional Annotation Tool (<http://david.abcc.ncifcrf.gov/>) following instructions. The GEO accession number for microarray data reported in this paper is GSE46672.

Salisphere and cell culture. Sorted cells were suspended in DMEM/F12 medium supplemented with 10% FBS, N2, B27, EGF (20 ng/ml), FGF2 (10 ng/ml) and IGF-1 (50 ng/ml), penicillin (100 U/ml), and streptomycin (100 mg/ml) (Gibco; Invitrogen), and then plated on Matrigel (BD Biosciences) in 96-well plates. Medium change was performed every other day. Salisphere numbers were counted on D7 and D14 of culture.

For in vitro passaging, D7 salispheres were released from Matrigel by Dispase (BD Biosciences) treatment for 30 minutes at 37°C, followed by 0.25% trypsin/EDTA for 3 minutes at 37°C, then passing through a 25-gauge needle 3 to 5 times. Single cells were counted under microscope and then plated again on a Matrigel 96-well plate.

Rat submandibular epithelial cell line SMG-C6 was obtained from Robert Castro (Neonatal and Developmental Medicine, Stanford University) and Margarita M. Vasquez (Neonatal Medicine, University of Texas Health Science Center, San Antonio, Texas, USA). Cells were cultured in DMEM/F12 medium as previously reported (78).

For additional information, see Supplemental Methods.

Statistics. Data were expressed as SEM. Statistical ANOVA and Student's *t* tests (2-tailed) were used to compare the data. $P \leq 0.05$ is considered to be significant.

Study approval. All animal procedures were approved by the Institutional Animal Care and Use Committee at Stanford University. Patient samples were collected via a protocol approved by the Stanford Institutional Review Board (IRB #17757).

Acknowledgments

This work was supported by grants from the NIH (R21DE021167A1-01 to Q.T. Le, H. Cao, and N. Xiao; 5P01CA067166-15 to Q.T. Le, D. Sirjani, A. Giaccia, and A. Koong). We thank Xuhuai Ji (Stanford University) and Shirley Kwok (Stanford University) for technical support, and Robert Castro (Stanford University) and Margarita M. Vasquez (University of Texas Health Science Center) for sharing the SMG-C6 cell line.

Address correspondence to: Quynh-Thu Le, Department of Radiation Oncology, 875 Blake Wilbur Dr., MC 5847, Stanford, California 94305-5847, USA. Phone: 650.725.0203; E-mail: qle@stanford.edu. Or to: Maximilian Diehn, Institute for Stem Cell Biology and Regenerative Medicine, 265 Campus Drive, R. G2120A, Stanford, California 94305, USA. Phone: 650.721.1550; E-mail: diehn@stanford.edu. Or to: Nan Xiao, Department of Radiation Oncology, 269 Campus Drive, CCSR South R. 1230, Stanford, California 94305, USA. Phone: 650.725.7805; E-mail: torixn@stanford.edu.

- Jemal A, Siegel R, Xu J, Ward E. Cancer statistics, 2010. *CA Cancer J Clin.* 2010;60(5):277-300.
- Cotrim AP, et al. Kinetics of tempol for prevention of xerostomia following head and neck irradiation in a mouse model. *Clin Cancer Res.* 2005;11(20):7564-7568.

- Lee NY, Le QT. New developments in radiation therapy for head and neck cancer: intensity-modulated radiation therapy and hypoxia targeting. *Semin Oncol.* 2008;35(3):236-250.
- Sagowski C, Wenzel S, Metternich FU, Kehrl W. Studies on the radioprotective potency of amifos-

- tine on salivary glands of rats during fractionated irradiation: acute and late effects. *Eur Arch Otorhinolaryngol.* 2003;260(1):42-47.
- Lombaert IM, et al. Rescue of salivary gland function after stem cell transplantation in irradiated glands. *PLoS One.* 2008;3(4):e2063.

6. Feng J, van der Zwaag M, Stokman MA, van Os R, Coppes RP. Isolation and characterization of human salivary gland cells for stem cell transplantation to reduce radiation-induced hyposalivation. *Radiother Oncol*. 2009;92(3):466–471.
7. Tran SD, Sumita Y, Khalili S. Bone marrow-derived cells: A potential approach for the treatment of xerostomia. *Int J Biochem Cell Biol*. 2011;43(1):5–9.
8. Sato A, et al. Isolation, tissue localization, and cellular characterization of progenitors derived from adult human salivary glands. *Cloning Stem Cells*. 2007;9(2):191–205.
9. David R, Shai E, Aframian DJ, Palmon A. Isolation and cultivation of integrin $\alpha 6 \beta 1$ -expressing salivary gland graft cells: a model for use with an artificial salivary gland. *Tissue Eng Part A*. 2008;14(2):331–337.
10. Baek H, Noh YH, Lee JH, Yeon SI, Jeong J, Kwon H. Autonomous isolation, long-term culture and differentiation potential of adult salivary gland-derived stem/progenitor cells [published online ahead of print August 23, 2012]. *J Tissue Eng Regen Med*. doi:10.1002/term.1572.
11. Banh A, et al. A novel aldehyde dehydrogenase-3 activator leads to adult salivary stem cell enrichment in vivo. *Clin Cancer Res*. 2011;17(23):7265–7272.
12. Saha K, Jaenisch R. Technical challenges in using human induced pluripotent stem cells to model disease. *Cell Stem Cell*. 2009;5(6):584–595.
13. Sariola H, Saarna M. Novel functions and signaling pathways for GDNF. *J Cell Sci*. 2003;116(pt 19):3855–3862.
14. Airaksinen MS, Saarna M. The GDNF family: signalling, biological functions and therapeutic value. *Nat Rev Neurosci*. 2002;3(5):383–394.
15. Lin LF, Doherty DH, Lile JD, Bektesh S, Collins F. GDNF: a glial cell line-derived neurotrophic factor for midbrain dopaminergic neurons. *Science*. 1993;260(5111):1130–1132.
16. Sainio K, et al. Glial-cell-line-derived neurotrophic factor is required for bud initiation from ureteric epithelium. *Development*. 1997;124(20):4077–4087.
17. Meng X, et al. Regulation of cell fate decision of undifferentiated spermatogonia by GDNF. *Science*. 2000;287(5457):1489–1493.
18. Peterson AL, Nutt JG. Treatment of Parkinson's disease with trophic factors. *Neurotherapeutics*. 2008;5(2):270–280.
19. Kirik D, Georgievska B, Bjorklund A. Localized striatal delivery of GDNF as a treatment for Parkinson disease. *Nat Neurosci*. 2004;7(2):105–110.
20. Saito Y, Ishikawa F. The origins of blood: induction of hematopoietic stem cells from different sources. *Cell Stem Cell*. 2008;3(1):8–10.
21. Takakura N, et al. A role for hematopoietic stem cells in promoting angiogenesis. *Cell*. 2000;102(2):199–209.
22. Radisky DC, LaBarge MA. Epithelial-mesenchymal transition and the stem cell phenotype. *Cell Stem Cell*. 2008;2(6):511–512.
23. Gonzalez B, Denzel S, Mack B, Conrad M, Gires O. EpCAM is involved in maintenance of the murine embryonic stem cell phenotype. *Stem Cells*. 2009;27(8):1782–1791.
24. Loffredo FS, Steinhilber ML, Gannon J, Lee RT. Bone marrow-derived cell therapy stimulates endogenous cardiomyocyte progenitors and promotes cardiac repair. *Cell Stem Cell*. 2011;8(4):389–398.
25. Matthews W, Jordan CT, Wiegand GW, Pardoll D, Lemischka IR. A receptor tyrosine kinase specific to hematopoietic stem and progenitor cell-enriched populations. *Cell*. 1991;65(7):1143–1152.
26. Wilson A, et al. Hematopoietic stem cells reversibly switch from dormancy to self-renewal during homeostasis and repair. *Cell*. 2008;135(6):1118–1129.
27. Matsumoto S, et al. Isolation of tissue progenitor cells from duct-ligated salivary glands of swine. *Cloning Stem Cells*. 2007;9(2):176–190.
28. Kingston R, Jenkinson EJ, Owen JJ. A single stem cell can recolonize an embryonic thymus, producing phenotypically distinct T-cell populations. *Nature*. 1985;317(6040):811–813.
29. Lombaert IM, Knox SM, Hoffman MP. Salivary gland progenitor cell biology provides a rationale for therapeutic salivary gland regeneration. *Oral Dis*. 2011;17(5):445–449.
30. Bickenbach JR. Isolation, characterization, and culture of epithelial stem cells. *Methods Mol Biol*. 2005;289:97–102.
31. Larsen HS, Aure MH, Peters SB, Larsen M, Messelt EB, Kanli Galtung H. Localization of AQP5 during development of the mouse submandibular salivary gland. *J Mol Histol*. 2011;42(1):71–81.
32. Stingl J, Eaves CJ, Zandieh I, Emerman JT. Characterization of bipotent mammary epithelial progenitor cells in normal adult human breast tissue. *Breast Cancer Res Treat*. 2001;67(2):93–109.
33. Villegas SN, Njaine B, Linden R, Carri NG. Glial-derived neurotrophic factor (GDNF) prevents ethanol (EtOH) induced B92 glial cell death by both PI3K/AKT and MEK/ERK signaling pathways. *Brain Res Bull*. 2006;71(1–3):116–126.
34. McAlhany RE, McAlhany RE Jr, West JR, Miranda RC. Glial-derived neurotrophic factor (GDNF) prevents ethanol-induced apoptosis and JUN kinase phosphorylation. *Brain Res Dev Brain Res*. 2000;119(2):209–216.
35. Tang MJ, Cai Y, Tsai SJ, Wang YK, Dressler GR. Ureteric bud outgrowth in response to RET activation is mediated by phosphatidylinositol 3-kinase. *Dev Biol*. 2002;243(1):128–136.
36. Jain S, Encinas M, Johnson EM, Johnson EM Jr, Milbrandt J. Critical and distinct roles for key RET tyrosine docking sites in renal development. *Genes Dev*. 2006;20(3):321–333.
37. Oatley JM, Avarbock MR, Brinster RL. Glial cell line-derived neurotrophic factor regulation of genes essential for self-renewal of mouse spermatogonial stem cells is dependent on Src family kinase signaling. *J Biol Chem*. 2007;282(35):25842–25851.
38. Euteneuer S, et al. Glial cell line-derived neurotrophic factor (GDNF) induces neurogenesis in the cochlear spiral ganglion via neural cell adhesion molecule (NCAM). *Mol Cell Neurosci*. 2013;54:30–43.
39. Charoy C, et al. gdnf activates midline repulsion by Semaphorin3B via NCAM during commissural axon guidance. *Neuron*. 2012;75(6):1051–1066.
40. Paratcha G, Ledda F, Ibanez CF. The neural cell adhesion molecule NCAM is an alternative signaling receptor for GDNF family ligands. *Cell*. 2003;113(7):867–879.
41. You L, Ebner S, Kruse FE. Glial cell-derived neurotrophic factor (GDNF)-induced migration and signal transduction in corneal epithelial cells. *Invest Ophthalmol Vis Sci*. 2001;42(11):2496–2504.
42. Barker N, Bartfeld S, Clevers H. Tissue-resident adult stem cell populations of rapidly self-renewing organs. *Cell Stem Cell*. 2010;7(6):656–670.
43. Pringle S, Nanduri LS, van der Zwaag M, van Os R, Coppes RP. Isolation of mouse salivary gland stem cells. *J Vis Exp*. 2011;(48):2484.
44. Lin CY, Lee BS, Liao CC, Cheng WJ, Chang FM, Chen MH. Transdifferentiation of bone marrow stem cells into acinar cells using a double chamber system. *J Formos Med Assoc*. 2007;106(1):1–7.
45. Lombaert IM, Wierenga PK, Kok T, Kampinga HH, deHaan G, Coppes RP. Mobilization of bone marrow stem cells by granulocyte colony-stimulating factor ameliorates radiation-induced damage to salivary glands. *Clin Cancer Res*. 2006;12(6):1804–1812.
46. Sumita Y, et al. Bone marrow-derived cells rescue salivary gland function in mice with head and neck irradiation. *Int J Biochem Cell Biol*. 2011;43(1):80–87.
47. Tran SD, et al. Microchimerism in salivary glands after blood- and marrow-derived stem cell transplantation. *Biol Blood Marrow Transplant*. 2011;17(3):429–433.
48. Sumita Y, et al. Bone marrow-derived cells rescue salivary gland function in mice with head and neck irradiation. *Int J Biochem Cell Biol*. 2011;43(1):80–87.
49. Lim JY, et al. Intraglandular transplantation of bone marrow-derived clonal mesenchymal stem cells for amelioration of post-irradiation salivary gland damage. *Oral Oncol*. 2013;49(2):136–143.
50. Maria OM, Tran SD. Human mesenchymal stem cells cultured with salivary gland biopsies adopt an epithelial phenotype. *Stem Cells Dev*. 2011;20(6):959–967.
51. Gorjup E, et al. Glandular tissue from human pancreas and salivary gland yields similar stem cell populations. *Eur J Cell Biol*. 2009;88(7):409–421.
52. Mishima K, et al. Transplantation of side population cells restores the function of damaged exocrine glands through clusterin. *Stem Cells*. 2012;30(9):1925–1937.
53. Blanpain C, Horsley V, Fuchs E. Epithelial stem cells: turning over new leaves. *Cell*. 2007;128(3):445–458.
54. Hai B, et al. Wnt/ β -catenin signaling regulates postnatal development and regeneration of the salivary gland. *Stem Cells Dev*. 2010;19(11):1793–1801.
55. Fiaschi M, Kolterud A, Nilsson M, Toftgard R, Rozell B. Targeted expression of GLI1 in the salivary glands results in an altered differentiation program and hyperplasia. *Am J Pathol*. 2011;179(5):2569–2579.
56. Dang H, Lin AL, Zhang B, Zhang HM, Katz MS, Yeh CK. Role for Notch signaling in salivary acinar cell growth and differentiation. *Dev Dyn*. 2009;238(3):724–731.
57. Arany S, Catalan MA, Roztocil E, Ovit CE. Ascl3 knockout and cell ablation models reveal complexity of salivary gland maintenance and regeneration. *Dev Biol*. 2011;353(2):186–193.

58. Musselmann K, et al. Salivary gland gene expression atlas identifies a new regulator of branching morphogenesis. *J Dent Res*. 2011;90(9):1078-1084.
59. Li L, Xie T. Stem cell niche: structure and function. *Annu Rev Cell Dev Biol*. 2005;21:605-631.
60. Harunaga J, Hsu JC, Yamada KM. Dynamics of salivary gland morphogenesis. *J Dent Res*. 2011;90(9):1070-1077.
61. Lombaert IM, Brunsting JF, Wierenga PK, Kampinga HH, de Haan G, Coppes RP. Keratinocyte growth factor prevents radiation damage to salivary glands by expansion of the stem/progenitor pool. *Stem Cells*. 2008;26(10):2595-2601.
62. Patel VN, et al. Specific heparan sulfate structures modulate FGF10-mediated submandibular gland epithelial morphogenesis and differentiation. *J Biol Chem*. 2008;283(14):9308-9317.
63. Jaskoll T, et al. FGF10/FGFR2b signaling plays essential roles during in vivo embryonic submandibular salivary gland morphogenesis. *BMC Dev Biol*. 2005;5:11.
64. Rebutini IT, Hoffman MP. ECM and FGF-dependent assay of embryonic SMG epithelial morphogenesis: investigating growth factor/matrix regulation of gene expression during submandibular gland development. *Methods Mol Biol*. 2009;522:319-330.
65. Knox SM, Lombaert IM, Reed X, Vitale-Cross L, Gutkind JS, Hoffman MP. Parasympathetic innervation maintains epithelial progenitor cells during salivary organogenesis. *Science*. 2010;329(5999):1645-1647.
66. Cawthorn WP, et al. Wnt6, Wnt10a and Wnt10b inhibit adipogenesis and stimulate osteoblastogenesis through a beta-catenin-dependent mechanism. *Bone*. 2012;50(2):477-489.
67. Krawetz R, Kelly GM. Wnt6 induces the specification and epithelialization of F9 embryonal carcinoma cells to primitive endoderm. *Cell Signal*. 2008;20(3):506-517.
68. Pruszk J, Sonntag KC, Aung MH, Sanchez-Pernaute R, Isacson O. Markers and methods for cell sorting of human embryonic stem cell-derived neural cell populations. *Stem Cells*. 2007;25(9):2257-2268.
69. Iso Y, et al. Distinct mobilization of circulating CD271+ mesenchymal progenitors from hematopoietic progenitors during aging and after myocardial infarction. *Stem Cells Transl Med*. 2012;1(6):462-468.
70. Xiao J, et al. Adipogenic and osteogenic differentiation of Lin(-)CD271(+)Sca-1(+) adipose-derived stem cells. *Mol Cell Biochem*. 2013;377(1-2):107-119.
71. Alam H, Sehgal L, Kundu ST, Dalal SN, Vaidya MM. Novel function of keratins 5 and 14 in proliferation and differentiation of stratified epithelial cells. *Mol Biol Cell*. 2011;22(21):4068-4078.
72. Al-Refu K, Edward S, Ingham E, Goodfield M. Expression of hair follicle stem cells detected by cytokeratin 15 stain: implications for pathogenesis of the scarring process in cutaneous lupus erythematosus. *Br J Dermatol*. 2009;160(6):1188-1196.
73. Troy TC, Turksen K. In vitro characteristics of early epidermal progenitors isolated from keratin 14 (K14)-deficient mice: insights into the role of keratin 17 in mouse keratinocytes. *J Cell Physiol*. 1999;180(3):409-421.
74. Knox SM, et al. Parasympathetic stimulation improves epithelial organ regeneration. *Nat Commun*. 2013;4:1494.
75. Livet J, et al. ETS gene Pea3 controls the central position and terminal arborization of specific motor neuron pools. *Neuron*. 2002;35(5):877-892.
76. Lu BC, et al. Etv4 and Etv5 are required downstream of GDNF and Ret for kidney branching morphogenesis. *Nat Genet*. 2009;41(12):1295-1302.
77. Chen C, et al. ERM is required for transcriptional control of the spermatogonial stem cell niche. *Nature*. 2005;436(7053):1030-1034.
78. Vasquez MM, Mustafa SB, Choudary A, Seidner SR, Castro R. Regulation of epithelial Na⁺ channel (ENaC) in the salivary cell line SMG-C6. *Exp Biol Med*. 2009;234(5):522-531.